2020 IEEE/RSJ International Conference on Intelligent Robots and Systems (IROS)
October 25-29, 2020, Las Vegas, NV, USA (Virtual)

Simultaneous 3D Forming and Patterning Method of Realizing Soft IPMC Robots

Keita Kubo[1], Hiroyuki Nabae[1], Tetsuya Horiuchi[2], Kinji Asaka[2], Gen Endo[1] and Koichi Suzumori[1]

***Abstract*— Ionic polymer-metal composites (IPMC) actuators are popular because they can be driven at a low voltage, possess excellent responsiveness, and can perform soft motions similar to that of living creatures. Conventional IPMC soft robots are manufactured by cutting and assembling IPMC sheets. However, using this conventional process to stably manufacture three-dimensional (3D)-shaped soft robots is difficult. To mitigate this problem, we propose a new method for fabricating 3D IPMC actuators in which several surface electrodes are separately fabricated from a single ion-exchange membrane. We refer to our proposal as the simultaneous 3D forming and patterning (SFP) method. Unlike the conventional IPMC fabrication process, the SFP method requires only one step to fix the ion-exchange membrane to contact masks. First, we briefly describe IPMC actuators, before introducing the proposed SFP method in detail. Next, we describe our investigations of the patterning resolution for the surface electrode using the proposed method. We fabricated two soft robot prototypes using the proposed method. The first robot is a starfish-type soft robot. Its surface electrode can be patterned in a plane using the proposed method, and independent driving is possible by applying voltage individually to the divided electrodes. The second prototype is a sea anemone-type soft robot, wherein surface electrodes can be patterned on a 3D curved surface to form a 3D shape.**

***Index Terms*— Soft Robot Applications, Soft Robot Materials and Design, Soft Sensors and Actuators**

I. INTRODUCTION

In recent years, there has been significant research related to soft robots. There are different types of flexible actuators that drive these soft robots, such as elastic fluidic, electro active polymer, and magnetically responsive soft actuators [1]. In particular, polymer actuators are garnering attention because they can save energy and perform biologically soft operations. In addition, they have the potential for mass production with inexpensive processes such as casting and pressing. One typical polymer actuator, the ionic polymer-metal composites (IPMC) actuator, is structured such that an ion-exchange membrane and a metal electrode are joined, as illustrated in Fig.1. When a voltage is applied to the surface electrode, it bends towards the anode [2] [3]. IPMC actuators can be driven at a low voltage (less than 5 V), with high response speeds (within 0.1 s) and a large displacement (90-degree bending angle) [4]. Moreover, they do not produce noise, and they can operate under water [5] [6]. Therefore, biomimetic robots such as fish- and snake-like robots have been developed using IPMCs [7]–[10]. Conventionally developed soft IPMC robots are mainly fabricated by cutting and pasting a commercially available sheet-shaped IPMC manufactured via rolling. Therefore, an assembly process is required to achieve complicated 3D operations. This is a problem because it is difficult to stably fabricate 3D IPMC robots.

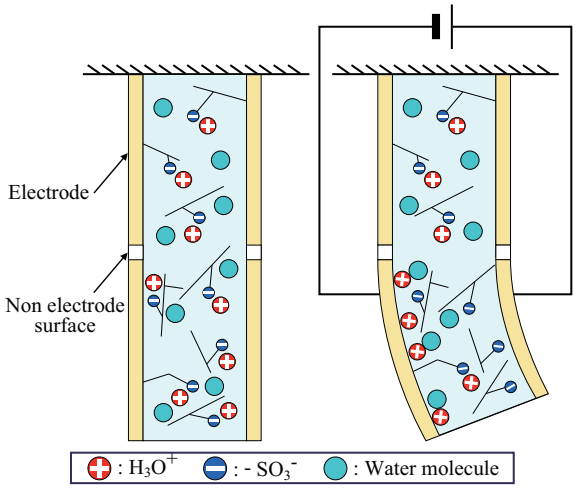

Fig. 1. Schematics and driving principles of patterned IPMC actuators.

Two approaches have been previously proposed to solve this problem. The first approach is to achieve 3D operations by constructing 3D IPMC structures. Previous approaches primarily use a 3D printer to generate 3D shapes [11]–[13]. Further, two other approaches are studied: the multi-layer casting process, which can create a thickness distribution in IPMC, though it has limitations [14], and shape memory effects, which can fabricate 3D shaped IPMCs using an elastic modulus whose value decreases with increasing temperature [15]. A 3D structure can be easily formed from 3D printing, but thermal deformation tends to occur owing to the characteristics of fused deposition modeling of 3D printers. This makes it difficult to produce micro-shapes or thin robots. Meanwhile, the fabrication process using shape memory effects is suitable for micro-shapes or thin IPMC robots because the shaped IPMC needs to be only heated and cooled.

The second approach is to divide the surface electrode of the IPMC into multiple areas and subsequently selectively

This work was supported by a Grant-in-Aid for Scientific Research in Innovative Areas under the "Science of Soft Robots" project funded by JSPS, grant number 18H05470.

[1]K. Kubo, H. Nabae, G. Endo, and K. Suzumori are with the School of Engineering, Tokyo Institute of Technology, 2-12-1 Ookayama, Meguro-ku, Tokyo 152-8550, Japan.

[2]T. Horiuchi and K. Asaka are with the National Institute of Advanced Industrial Science and Technology, Osaka 563-8577, Japan.

drive these to achieve complex operations. Surface electrode patterning is also effective in counteracting the relaxation effect, a unique feature of IPMC [16]. There are several available separation methods: burning the surface electrode using a laser, mechanically cutting the surface electrode, shaving the surface electrode through etching, lithography, and pasting tape on part of the ion-exchange membrane surface when plating the surface electrode [17]–[20]. Laser cutting, machining, and lithography are highly reliable because they cut part of the already plated surface, although these methods are difficult to apply to 3D curved surfaces. Though unreliable, the tape method can be applied to a curved surface because the tape can peel off during plating and it is difficult to attach micro-patterns.

Therefore, we propose a method known as simultaneous 3D forming and patterning (SFP) that can form 3D-shaped IPMC structures and fabricate electrodes selectively and reliably for 3D curved surfaces. The SFP method can integrally fabricate an IPMC soft robot with a 3D structure on which the surface electrodes are patterned. Furthermore, the proposed method can be used to fabricate soft robots from one ion-exchange membrane by keeping the membrane in close contact with contact masks when plating the surface electrodes. The method is simple and safe because, unlike existing methods, it adds only one step of sandwiching and fixing the ion-exchange membrane to contact masks. The SFP method can simultaneously form a 3D shape and pattern the electrodes, thus contributing to the realization of more complex and multi-degree-of-freedom IPMC robots. In this paper, we introduce and evaluate the proposed method, and we demonstrate its effectiveness by describing the fabrication of two soft robots.

II. SIMULTANEOUS 3D FORMING AND PATTERNING METHOD

In this section, we describe the proposed SFP method.

A. Outline of SFP method

The SFP method is approximately divided into three steps: the masking and fixing process, the electroless plating process, and the removal of any extra areas. A flowchart is presented in Fig.2. All the IPMCs described below were fabricated from a single Nafion membrane using the cast method [21]. Fig.3 illustrates the appearance of a Nafion membrane. The following subsections detail the masking and fixing process, which is the main part of the proposed SFP method, and the previously proposed electroless plating process.

B. Masking and fixing process

This process is the main process of the proposed SFP method. The masking and fixing process is divided into the following four steps:

1) Make a contact mask made of resin using a 3D printer or NC processing machine.
2) Next, soak the Nafion sheet in pure water and swell it in advance.

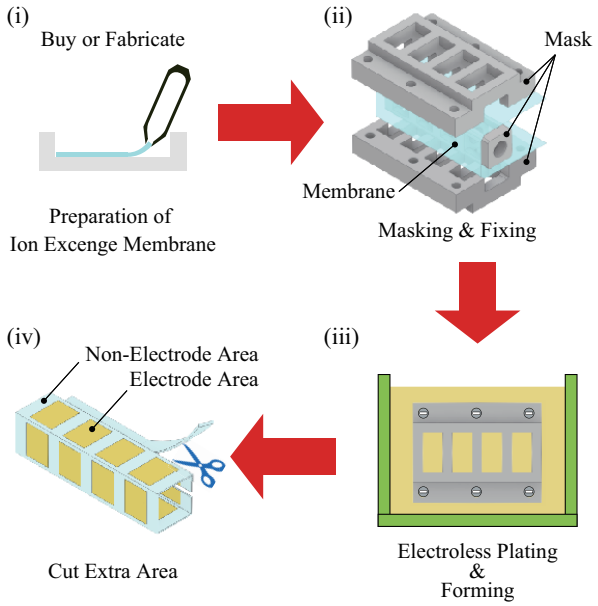

Fig. 2. Fabrication process: (i) preparation of ion-exchange membrane; (ii) masking and fixing process of the SFP method; (iii) electroless plating process; (iv) removal of extra area.

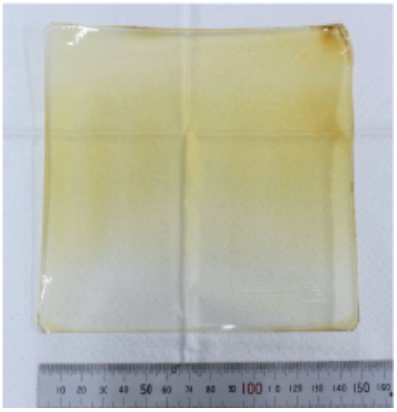

Fig. 3. Nafion membrane fabricated using the cast method.

3) Subsequently, insert the Nafion sheet between the masks.
4) Finally, fix the masks and the Nafion sheet using resin screws.

The contact mask comprises penetrating parts for electrode deposition, masks that prevent electrode deposition from contacting the membrane, and structural parts that do not directly contact the membrane. A schematic diagram of the patterning principle of the proposed method is presented in Fig.4. In the electroless plating process described below, the Nafion adsorbs the gold complex, and gold is deposited on the surface through reduction. This does not occur unless each solution and the Nafion membrane are in direct contact. In other words, the part that is in contact with the contact mask does not come into direct contact with any solution. Therefore, neither adsorption nor reduction occurs,

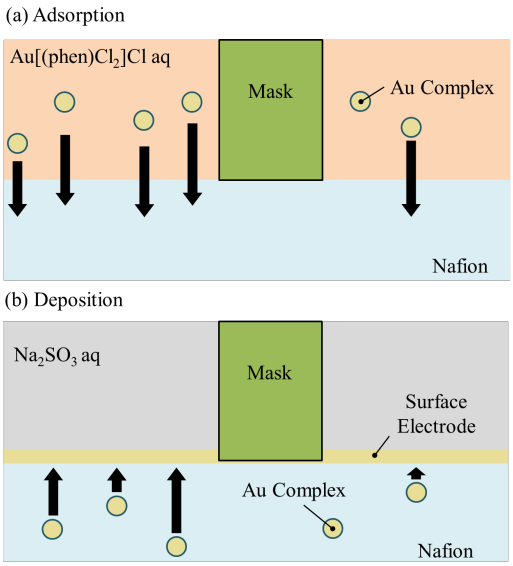

Fig. 4. Masking principle.

and no electrode is deposited. This enables the patterning to selectively produce electrodes on the Nafion surface. When 3D-shaped contact masks are used, the shape of the Nafion membrane when plating the electrode is maintained even after removing the masks. This enables 3D forming, similar to 2D-shaped masks used to produce IPMCs with a planar shape. The Nafion membrane often curls during the electroless plating process; thus, this method is effective in that it can be used to fabricate IPMC soft robots that will not lose their 2D shape. 3D forming performed by heating IPMC to 60 ˚ C in the electroless plating process. Subsequently, the shape of the IPMC is fixed by cooling it at room temperature using water.

The second step of the masking and fixing processes is a relatively important operation. Nafion membranes absorb, and this water is stored inside them and can lead to swelling. Therefore, when a dried Nafion membrane is fixed to the contact mask before the electroless plating process is performed, differences in the swelling of the membrane between the penetrated parts of the contact mask and the mask cause the Nafion membrane to wrinkle at the penetrated parts when soaked in the solution. We also discuss the failure mode of the SFP method. It has been confirmed that electrode patterning failure occurs when the resin screw that fixes the mask is loosely fastened or there is a significant variation in the fastening force. However, this can be avoided by using a torque driver or masks that do not easily affect the fastening force on the fixation of the polymer.

C. Electroless plating and forming process

The electroless plating process, developed by Fujiwara et al., was used to bond the electrodes to the fabricated Nafion membrane [22]. This has been used as a method of fabricating IPMCs. The process is divided into the following three steps:

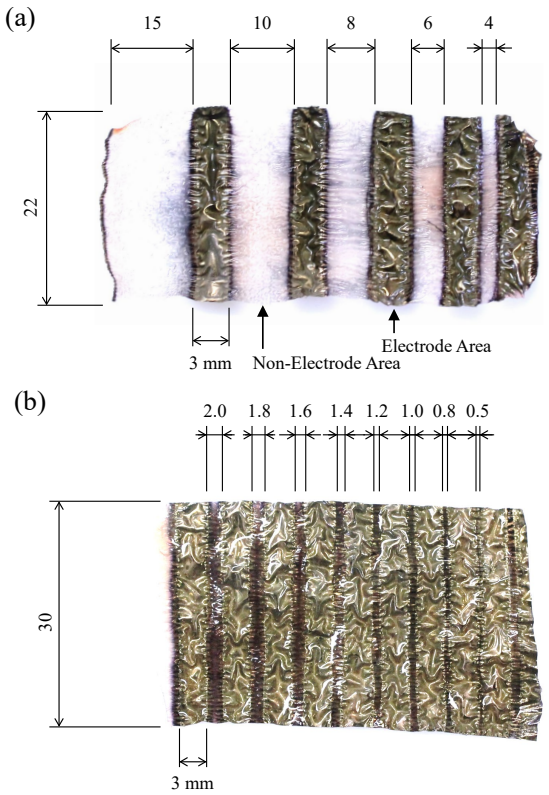

Fig. 5. Electrode patterning test: (i) the distance between the electrodes is 15–4 mm; (ii) the distance between the electrodes is 2.0–0.5 mm.

1) A Nafion membrane fixed with a contact mask is immersed overnight in a gold complex aqueous solution at room temperature such that the membrane adsorbs the gold complex ($\mathrm{Au[(phen)Cl_2]Cl\,aq}$).
2) It is soaked in a reducing agent solution ($\mathrm{Na_2SO_3\,aq}$) at $60°\mathrm{C}$ for 3.5 h to deposit the gold on the surface.
3) The membrane is washed by immersing it in deionized water at $40°\mathrm{C}$.

This process is repeated until the surface resistance of the electrode reaches several Ω.

III. PATTERNING RESOLUTION TEST

When electroless plating is performed, the reducing agent slightly penetrates the surface of the Nafion membrane that is in close contact with the contact mask. To investigate the limit of the mask width required for patterning the surface electrodes, we fabricated IPMCs for the patterning test illustrated in Fig.5. As illustrated in Fig.5, the electrodes and non-electrode parts could be visually distinguished using a wide mask. When the distance between the electrodes was less than 2.0 mm, however, the non-electrode parts were slightly plated with gold, and no separation of the electrodes could be visually confirmed. Therefore, we quantitatively evaluated the patterning performance by measuring the impedance between adjacent electrodes. We used impedance as a measure of insulation to drive the IPMC robot using an alternating current (AC). The measurement was performed

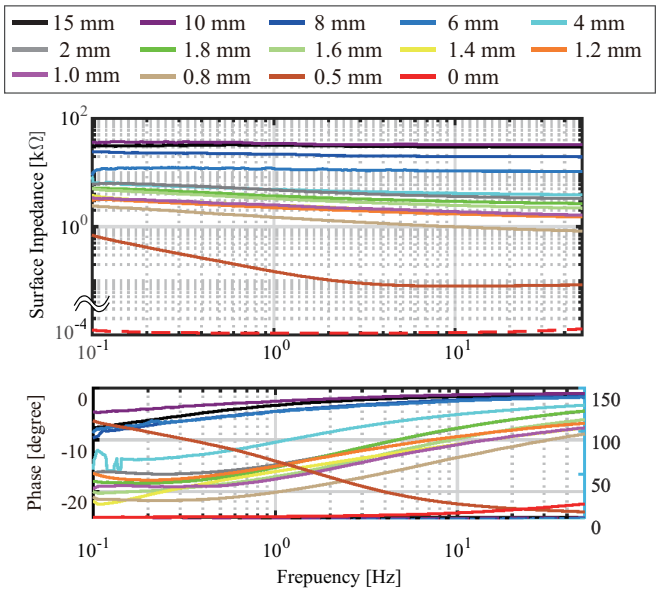

Fig. 6. Nafion surface impedance between adjacent electrodes.

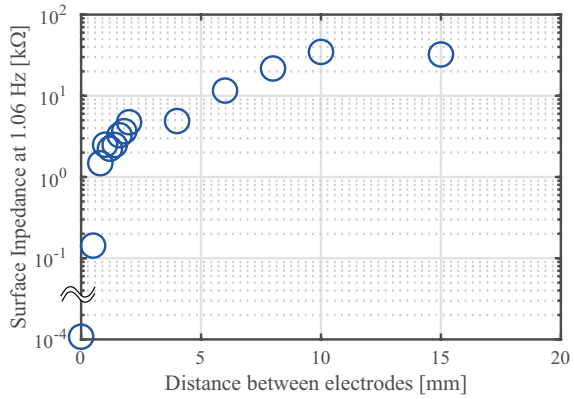

Fig. 7. Nafion surface impedance between adjacent electrodes at 1.06 Hz.

using a chemical impedance analyzer (IM3590, manufactured by Hioki Co. Ltd.). Fig.6 demonstrates the relationship between the distance between adjacent electrodes and the impedance measured in the frequency range from 0.1 to 50 Hz. Similarly, Fig.7 demonstrates the relationship between the impedance and the distance between adjacent electrodes at a frequency of 1.06 Hz that is nearly equal to the actual frequency. From Fig.6, the impedance between the electrodes is directly proportional to the distance between adjacent electrodes. Regarding the phase, the data with the electrode distance of 0.5 mm and 0 mm tended to be different from other data; therefore, they were indicated on the second axis. Moreover, as illustrated in Fig.7, when the distance between the electrodes is less than 10 mm, the impedance simultaneously increases with the distance, but it is expected to be constant beyond 10 mm. The result indicates a discontinuity between the electrode distances of 4 mm and 2 mm. However, we considered that it was caused by individual differences of the IPMC because data less than 2 mm and greater than 4 mm were measured using a different IPMC as illustrated in Fig.5. IPMCs are driven using current; thus, they cannot be driven using voltage drops when there is a high surface resistance because there is a low impedance between electrodes facing each other. Therefore, IPMCs are usually designed such that the surface resistance of the actuator part (i.e., the electrode part) becomes several Ω. Based on the above-mentioned, even the minimum mask width (0.5 mm) of each electrode can be regarded as insulated. This is because the impedance between adjacent electrodes is several hundred Ω.

IV. APPLICATION TO SOFT ROBOTS

This section describes two soft IPMC robots that were fabricated using the proposed SFP method. The first robot is a starfish-type soft IPMC robot with a planar shape and patterned electrodes. From this prototype, we can demonstrate that the method can be used to pattern electrodes on a plane, forming a clean plane shape for a soft robot. The second robot is a sea anemone-type soft IPMC robot with a 3D shape and patterned electrodes on a curved surface. From this prototype, we can demonstrate electrode patterning on curved surfaces and the formation of 3D shapes. Both robots are not intended to imitate the movements of living things but are mentioned for their similarity in appearance.

A. *Starfish-type soft robot*

A starfish-type soft robot was fabricated to demonstrate patterned surface electrodes on a plane and a clean plane shape formed with the SFP method. Fig.8 shows the appearance of the fabricated IPMC, the assembled soft robot, and the mask. A starfish-type IPMC refers to a five-armed starfish, with five independent surface electrodes at the same position at the front and back. The starfish can move each of its five arms independently by applying a voltage to each pair of surface electrodes. The gold parts of the starfish-type IPMC, illustrated in Fig.8(a), are electrode parts, and the transparent part denotes the non-electrode part. The thickness of the fabricated starfish-type IPMC is approximately 109 μ m at the non-electrode part. Unintended electrode deposition was observed in the non-electrode part, which was considered to be from the permeation of the plating solution into the part where the contact was loose between the Nafion and the contact masks. This was because the thickness of the Nafion film produced by the casting method was not constant, and the masks deflected from the variation in the fastening force, owing to the manual fastening of the resin screw when fixing the masks. Regarding the insulation properties, it is considered that the influence on the driving was insignificant because the distances between the adjacent arm electrodes are greater than 4 mm. The starfish-type soft robot comprises a starfish-type IPMC, a thin metal plate with a back surface electrode as a common GND, and five additional electrodes that contact the front surface electrode, as illustrated in Fig.8(b). The contact masks were manufactured by milling

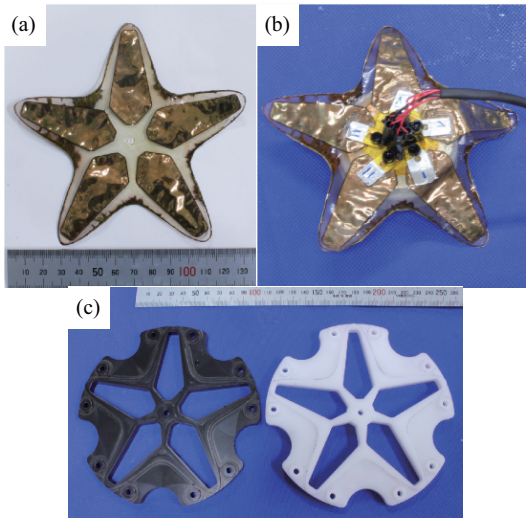

Fig. 8. Starfish-type IPMC soft robot and masks: (a) starfish-type IPMC fabricated from a Nafion membrane. The gold areas represent the electrode parts, whereas the clear area denotes the non-electrode parts; (b) starfish-type soft robot with five independent arms attached to the outer electrode to apply voltage; (c) contact masks used to fabricate the starfish-type IPMC with through the SFP method.

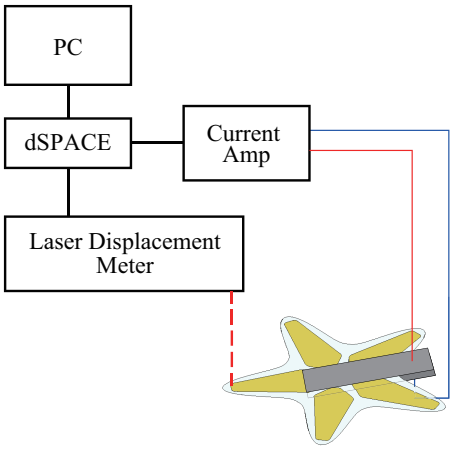

Fig. 9. Experimental setup for measuring the displacement of the starfish-type IPMC arm.

POM. As illustrated in Fig.8(c), the surface of the masks that come into contact with the Nafion is divided into a penetrating part where the electrode is deposited, a mask part that comes into contact with the membrane, and a structural part that does not come into direct contact.

In the experiment, the displacement was measured when applying a sine wave voltage of 3.8 V_{p-p} and offset of 0.6 V at 1 Hz to one of the arms. The soft robot was driven through converting a sine wave signal produced by a computer into an analog signal using dSPACE and applying the signal via a current amplifier. The displacement was measured using a laser displacement meter. The setup of the experimental environment is illustrated in Fig.9. The displacement response is presented in Fig.10. As illustrated in Fig.10, the center of the vibration of the arm displacement first shifted to the positive direction and subsequently returned to the negative direction, deviating from the initial displacement. When a DC voltage is applied to the IPMC, a relaxation effect occurs in which the IPMC is displaced in the opposite direction after bending. In this experiment, an offsetting AC voltage was applied. Thus, the results demonstrate this effect. Next, we conducted an experiment by changing the voltage such that the arbitrary voltage output from dSPACE via the current amplifier could be applied to each of the five arms by switching between them, on and off using a switch. The driving experiment is demonstrated in Fig.11. In the experiments in which the arms were moved individually, we succeeded in selectively driving up to three of the five legs. Therefore, we could drive with only one arm and with two or three different arms, simultaneously. When we drove each arm before attaching external electrodes, we confirmed their individual operations. However, we could not drive two arms after composing a soft robot. This failure is not caused by the proposed SFP method but by poor contact between the IPMC and external electrodes. The electrical connection between the external electrodes and the IPMC will be improved in future studies. Regarding the electrical connection between the IPMC and the external electrodes, Arena et al. proposed a method of embedding conductors when manufacturing an IPMC; we will consider this as a reference [23]. In addition, we will investigate the possibility of influencing IPMC robot designs in future studies because it cannot be denied that the application of a voltage to one arm may have invisible effects on another arm,.

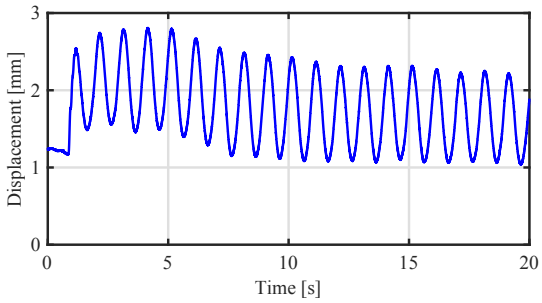

Fig. 10. Displacement of the starfish-type IPMC arm.

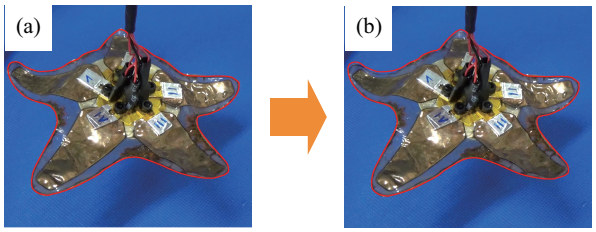

Fig. 11. Driving experiment of the starfish-type IPMC: (a) input voltage equal to 5 V; (b) input voltage equal to 0 V.

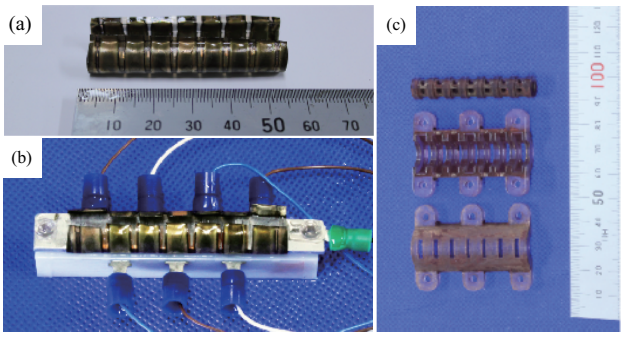

Fig. 12. Sea anemone-type IPMC soft robot with masks: (a) sea anemone-type IPMC fabricated from a Nafion membrane; (b) sea anemone-type soft robot; (c) contact masks used to fabricate the sea anemone-type IPMC through the SFP method. From the top: core supporting the membrane from the inside and patterned inner surface electrodes; inside view of the half cylinder; and outside view of the half cylinder.

B. Sea anemone-type robot

A cylindrical shape was adopted as a simple structure to demonstrate the creation of 3D shapes using the proposed SFP Method. We designed it as a sea anemone-type robot because it can be driven independently for each pair of left and right surface electrodes. The appearance of the mask used with the sea anemone-type robot is presented in Fig.12. The sea anemone-type IPMC has a cylindrical shape, and 4 mm-wide electrodes that make one round, arranged at a 7 mm pitch on the circumference. The cylindrical side does not circumvent once because of the fabrication of the prototype, but we used this shape for the driving parts. When making the sea anemone-type soft robot, cuts were made in the non-electrode part between each electrode part, and the electrode part was separated. As illustrated in Fig.12(b), the sea anemone-type robot is an IPMC with partly separated electrodes, metal electrodes for the inner surface electrodes of a common GND, and a 3D printed jig that holds the IPMC and the metal electrode, contacting the outer surface electrodes with the external electrode. The contact masks comprise two hollow semi-cylinders with holes on the sides and a core supporting the Nafion membrane from the inside. The hole on the side serves to prevent the plating failure of the electrode part by circulating the aqueous solution and reducing the solution of the gold complex through the hole in the electroless process.

First, experiments were conducted to determine the shape stability of the IPMC. In this experiment, we applied an external force to the sea anemone-type IPMC using a weight. Subsequently, we measured its deformation from the original shape after unloading using a laser displacement meter. For comparison, we conducted the same experiment with a sea anemone-shape Nafion without surface electrodes. It is formed by soaking in deionized water for the same duration and temperature as the electroless plating process. The experimental setup is illustrated in Fig.13. The result

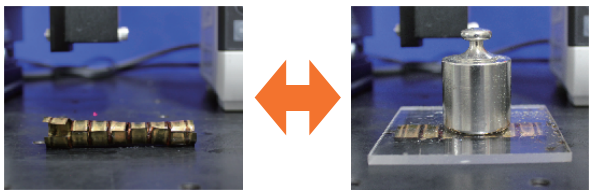

Fig. 13. Test to confirm that the sea anemone-type IPMC can retain its 3D form after loading and unloading.

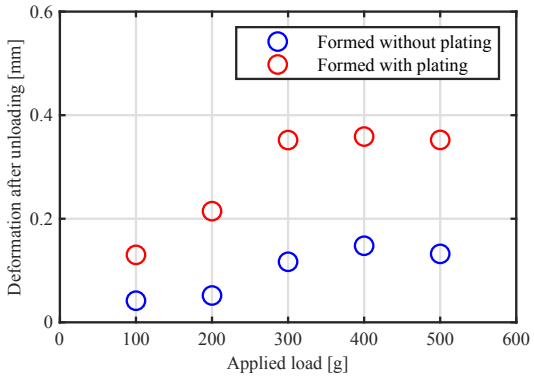

Fig. 14. Deformation of the IPMC formed with plating and without plating when a load is applied and then unloaded.

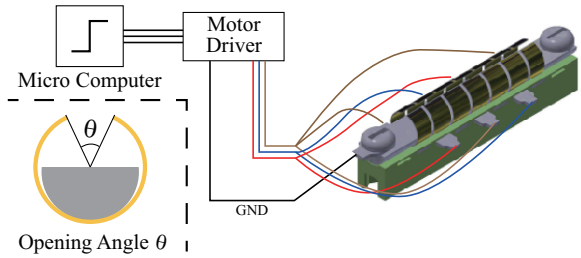

Fig. 15. Experimental setup to drive the sea anemone-type soft robot and definition of the opening angle θ.

is presented in Fig.14. According to Fig.14, the shape stability of the IPMC formed without plating is higher than that of the IPMC formed with plating. This is considered to be due to the plastic deformation of the surface gold electrodes of IPMC, whereas the Nafion is nearly elastically deformed. The deformations increased up to 300 g but remained constant thereafter. Next, we constructed a soft robot and performed an experiment. The experiment is demonstrated in Fig.15. The outer surface electrodes are connected in three groups, and a three-phase voltage can be applied from a microcomputer via a motor driver. In the experiment, we applied 5 V and 0.33 Hz three-phase square wave voltage to each electrode of the sea anemone-type soft robot. We also measured the opening angle of the IPMC. The result is presented in Fig.16. As illustrated in Fig.16, the frequency of the vibration is equal to that of the applied voltage. Additionally, the center of the vibration of the angle first shifted to the positive direction and then returned to the negative direction, similar to the starfish-type

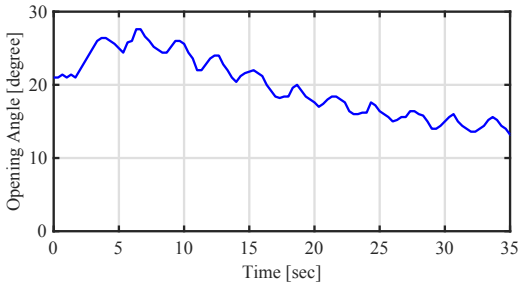

Fig. 16. Driving experiment result of the sea anemone-type soft robot.

soft robot. This was due to a similar reason, relaxation effect, because the applied voltage is 0 to 5 V square wave voltage. We also confirmed that the divided driving parts operate independently.

V. DISCUSSION

In this paper, we proposed the SFP method to improve the shape and design flexibility of IPMCs. IPMC actuators are difficult to apply to soft robots because they are conventionally fabricated through cutting and assembling. After describing the specific procedure of the SFP method, specific problems and solutions were presented. We fabricated an IPMC soft robot using the proposed method with a Nafion membrane fabricated through the cast method. Considering the principle of this method, we expect that it can be applied to any commercially available Nafion membrane. We will verify this in future studies. We also expect that this method can be used to fabricate IPMC soft robots of any desired shape from commercially available ion-exchange membranes without using 3D printing. In addition, we demonstrated that 3D forming is possible using the SFP method. We also investigated the resolution of the patterning, and confirmed that the impedance decreased as the inter-electrode distance decreased. Further, the phase of the impedance tended to differ from the phase of the inter-electrode distance of 0.8 mm or greater when the inter-electrode distance was 0.5 mm. We will investigate the cause of this in future studies. Finally, we fabricated a 2D starfish-type soft robot and a 3D sea anemone-type robot using the proposed method. The independent driving of the patterned electrodes was confirmed in each soft robot, and we demonstrated that the formed shape was retained when the load was removed after applying an external force. The IPMC soft robots that we produced had relatively simple structures. Clearly, they were prototypes merely intended to demonstrate the SFP method. In the future, we plan to implement artificial intelligence in our robots. We will pursue the fabrication of soft robots with more complicated structures, such as a mobile unit using a multi-degree-of-freedom manipulator.

VI. CONCLUSION

In this paper, we proposed the SFP method of forming 3D-shaped IPMCs from a single Nafion membrane while patterning the surface electrodes for the purpose of manufacturing IPMC soft robots. The proposed method results in fabrications of 3D-shaped IPMC robots with multiple degrees of freedom and without a mechanical assembly process. We described the SFP method in detail and validated it experimentally with two examples of IPMC robots.

1) SFP method was developed and demonstrated to be effective.
2) Soft IPMC robots were developed using the SFP method, and their driving parts could be individually actuated.
3) The SFP method can be applied to various shapes and geometries and simplify soft robotics fabrication.

REFERENCES

[1] L. Hines, K. Petersen, G. Z. Lum, and M. Sitti, "Soft actuators for small-scale robotics," *Advanced Materials*, vol. 29, no. 13, p. 1603483, 2017. [Online]. Available: https://onlinelibrary.wiley.com/doi/abs/10.1002/adma.201603483

[2] K. Oguro, Y. Kawami, and H. Takenaka, "Bending of an ion-conducting polymer film-electrode composite by an electric stimulus at low voltage," *J. Micromachine Society*, vol. 5, pp. 27–30, 1992.

[3] S. Nemat-Nasser and J. Y. Li, "Electromechanical response of ionic polymer-metal composites," *Journal of Applied Physics*, vol. 87, no. 7, pp. 3321–3331, 2000. [Online]. Available: https://doi.org/10.1063/1.372343

[4] M. Konyo and S. Tadokoro, *IPMC Based Tactile Displays for Pressure and Texture Presentation on a Human Finger*. John Wiley and Sons, Ltd, 2009, ch. 8, pp. 161–174. [Online]. Available: https://onlinelibrary.wiley.com/doi/abs/10.1002/9780470744697.ch8

[5] D. Pugal, K. Jung, A. Aabloo, and K. J. Kim, "Ionic polymer-metal composite mechanoelectrical transduction: review and perspectives," *Polymer International*, vol. 59, no. 3, pp. 279–289, Mar 2010. [Online]. Available: https://doi.org/10.1002/pi.2759

[6] K. Jung, J. Nam, and H. Choi, "Investigations on actuation characteristics of ipmc artificial muscle actuator," *Sensors and Actuators A: Physical*, vol. 107, no. 2, pp. 183 – 192, 2003. [Online]. Available: http://www.sciencedirect.com/science/article/pii/S0924424703003467

[7] S. Trabia, "Comprehensive study of spray-painting and 3d printing fabrication methods for nafion® and nafion® equivalents in ionic polymer-metal composite actuators and sensors," 2018.

[8] B. L. Stoimenov, J. Rossiter, and T. Mukai, "Soft ionic polymer metal composite (IPMC) robot swimming in viscous fluid," in *Electroactive Polymer Actuators and Devices (EAPAD) 2009*, Y. Bar-Cohen and T. Wallmersperger, Eds., vol. 7287, International Society for Optics and Photonics. SPIE, 2009, pp. 757 – 764. [Online]. Available: https://doi.org/10.1117/12.818705

[9] M. Yamakita, N. Kamamichi, T. Kozuki, K. Asaka, and Zhi-Wei Luo, "A snake-like swimming robot using ipmc actuator and verification of doping effect," in *2005 IEEE/RSJ International Conference on Intelligent Robots and Systems*, Aug 2005, pp. 2035–2040.

[10] Xiufen Ye, Yudong Su, and Shuxiang Guo, "A centimeter-scale autonomous robotic fish actuated by ipmc actuator," in *2007 IEEE International Conference on Robotics and Biomimetics (ROBIO)*, Dec 2007, pp. 262–267.

[11] J. D. Carrico, N. W. Traeden, M. Aureli, and K. K. Leang, "Fused filament 3d printing of ionic polymer-metal composites (IPMCs)," *Smart Materials and Structures*, vol. 24, no. 12, p. 125021, nov 2015.

[12] J. D. Carrico, K. J. Kim, and K. K. Leang, "3d-printed ionic polymer-metal composite soft crawling robot," in *2017 IEEE International Conference on Robotics and Automation (ICRA)*, May 2017, pp. 4313–4320.

[13] J. D. Carrico, T. Hermans, K. J. Kim, and K. K. Leang, "3d-printing and machine learning control of soft ionic polymer-metal composite actuators," *Scientific Reports*, vol. 9, no. 1, p. 17482, 2019. [Online]. Available: https://doi.org/10.1038/s41598-019-53570-y

[14] A. Kodaira, K. Asaka, T. Horiuchi, G. Endo, H. Nabae, and K. Suzumori, "Ipmc monolithic thin film robots fabricated using a multi-layer casting process," *IEEE Robotics and Automation Letters*, vol. 4, pp. 1335–1342, 2019.

[15] J. Rossiter, K. Takashima, and T. Mukai, "Shape memory properties of ionic polymer–metal composites," *Smart materials and structures*, vol. 21, no. 11, p. 112002, 2012.

[16] M. J. Fleming, K. K. Leang, and K. J. Kim, "Mitigating ipmc back relaxation through feedforward and feedback control of patterned electrodes," vol. 21, no. 8, p. 12, 2012. [Online]. Available: http://dx.doi.org/10.1088/0964-1726/21/8/085002

[17] Y. Nakabo, T. Mukai, and K. Asaka, "Biomimetic soft robots with artificial muscles," in *Smart Materials III*, A. R. Wilson, Ed., vol. 5648, International Society for Optics and Photonics. SPIE, 2004, pp. 132 – 144. [Online]. Available: https://doi.org/10.1117/12.581825

[18] M. Tsugawa, V. Palmre, J. Carrico, K. Kim, and K. Leang, "Slender tube-shaped and square rod-shaped ipmc actuators with integrated sensing for soft mechatronics," *Meccanica*, vol. 50, pp. 2781–2795, 06 2015.

[19] Z. Chen, "A review on robotic fish enabled by ionic polymer–metal composite artificial muscles," *Robotics and Biomimetics*, vol. 4, no. 1, p. 24, Dec 2017.

[20] W. Yanjie, C. Hualing, W. Yongquan, L. Jiayu, and L. Dichen, "Manufacturing process for patterned ipmc actuator with millimeter thickness," in *2013 IEEE International Symposium on Assembly and Manufacturing (ISAM)*, July 2013, pp. 235–239.

[21] S.-E. Cha, J.-H. Park, and S.-G. Lee, "Fabrication process and characterization of sonic polymer-metal composite actuators by electroless plating of platinum," *The Transactions of the Korean Institute of Electrical Engineers C*, vol. 51, no. 9, pp. 455–463, 2002.

[22] N. Fujiwara, K. Asaka, Y. Nishimura, K. Oguro, and E. Torikai, "Preparation of gold solid polymer electrolyte composites as electric stimuli-responsive materials," *Chemistry of Materials*, vol. 12, no. 6, pp. 1750–1754, 2000.

[23] P. Arena, C. Bonomo, L. Fortuna, M. Frasca, and S. Graziani, "Design and control of an ipmc wormlike robot," *IEEE Transactions on Systems, Man, and Cybernetics, Part B (Cybernetics)*, vol. 36, no. 5, pp. 1044–1052, Oct 2006.